



Low noise MgB2 hot electron bolometer mixer operated at 5.3 THz and at 20 K

Downloaded from: <https://research.chalmers.se>, 2025-12-04 23:29 UTC

Citation for the original published paper (version of record):

Gan, Y., Mirzaei, B., Silva, J. et al (2021). Low noise MgB2 hot electron bolometer mixer operated at 5.3 THz and at 20 K. Applied Physics Letters, 119(20). <http://dx.doi.org/10.1063/5.0070153>

N.B. When citing this work, cite the original published paper.

Low noise MgB_2 hot electron bolometer mixer operated at 5.3 THz and at 20 K

Cite as: Appl. Phys. Lett. **119**, 202601 (2021); doi: [10.1063/5.0070153](https://doi.org/10.1063/5.0070153)

Submitted: 4 September 2021 · Accepted: 1 November 2021 ·

Published Online: 17 November 2021



View Online



Export Citation



CrossMark

Y. Gan,^{1,2,a)} B. Mirzaei,^{1,3} J. R. G. D. Silva,^{1,2} J. Chang,³ S. Cherednichenko,⁴ F. van der Tak,^{1,2} and J. R. Gao^{1,3}

AFFILIATIONS

¹SRON Netherlands Institute for Space Research, Landleven 12, 9747 AD Groningen and Niels Bohrweg 4, 2333 CA Leiden, The Netherlands

²Kapteyn Astronomical Institute, University of Groningen, 9747 AD Groningen, The Netherlands

³Optics Group, Department of Imaging Physics, Delft University of Technology, 2628 CJ Delft, The Netherlands

⁴Terahertz and Millimetre Wave Laboratory, Department of Microtechnology and Nanoscience, Chalmers University of Technology, SE-412 96 Gothenburg, Sweden

^{a)} Author to whom correspondence should be addressed: Y.N.Gan@sron.nl

ABSTRACT

We have demonstrated a low noise superconducting MgB_2 hot electron bolometer (HEB) mixer working at the frequency of 5.3 terahertz (THz) with 20 K operation temperature. The bolometer consists of a 7 nm thick MgB_2 submicrometer bridge contacted with a spiral antenna to couple THz radiation through a high resistive Si lens, and it has a superconducting critical temperature of 38 K. By using hot/cold blackbody loads and a Mylar beam splitter all in vacuum and applying a 5.25 THz far-infrared gas laser as a local oscillator, we measured a minimal double sideband receiver noise temperature of 3960 K at the LO power of 9.5 μW . This can be further reduced to 2920 K if a Si lens with an antireflection coating optimized at this frequency and a 3 μm beam splitter are used. The measured intermediate frequency (IF) noise bandwidth is 9.5 GHz. The low noise, wide IF bandwidth mixers, which can be operated in a compact, low dissipation Stirling cooler, are more suitable for space applications than the existing HEB mixers. Furthermore, we likely observed a signature of the double-gap in MgB_2 by comparing current–voltage curves pumped at 5.3 and 1.6 THz.

Published under an exclusive license by AIP Publishing. <https://doi.org/10.1063/5.0070153>

Superconducting hot electron bolometer (HEB) mixers¹ are so far the most sensitive heterodyne detectors for high-resolution spectroscopy at frequencies between 1.2 and 6 terahertz (THz).² They play a key role in astrophysics at terahertz (THz) frequencies, as this range is rich in the atomic, ionic, and molecular spectral lines that can, for example, directly probe how star formation proceeds in galaxies.³ Such mixers have been successfully applied for the airborne telescope of Stratospheric Observatory for Infrared Astronomy,⁴ the balloon-borne telescope of Stratospheric Terahertz Observatory-2,⁵ and the space telescope of the Herschel Space Observatory.⁶

To date, HEB mixers based on thin NbN films have shown excellent sensitivities, where their double sideband receiver noise temperature ($T_{\text{rec}}^{\text{DSB}}$) is approaching seven times the quantum noise.⁷ However, one drawback of such mixers is their limited intermediate frequency (IF) bandwidth, typically below 4 GHz. Another restriction comes from the low operating temperature around 4 K due to their low critical temperature (T_c) of 8–10 K. Cooling down to 4 K, either by using

liquid He vessels or a mechanical pulse tube is suboptimal for a space observatory considering the constraints on mass, volume, electrical power, and cost. For example, for the next generation of THz observatories with a number of telescopes operated as an interferometer in space⁸ and the Earth atmospheric observations from space,⁹ the weight and consumed electrical power of cryo-coolers becomes much less if the operating temperature could be tolerated to 20 K or above.

Superconducting MgB_2 with a T_c of 40 K in bulk¹⁰ is considered as a candidate to increase the IF bandwidth of an HEB mixer and also the operating temperature. The first MgB_2 HEB mixer based on a molecular beam epitaxy (MBE) growth, 20 nm thick film with a T_c of 22 K was reported at 1.6 THz.¹¹ The HEB mixers based on hybrid physical chemical vapor deposition (HPCVD) growth MgB_2 films, 10–20 nm, with an increased T_c of 33–38 K were reported at 600 GHz.¹² An HEB mixer based on a MgB_2 film of 7 nm with a T_c of 34 K, milled from a thicker film by an Ar ion mill, was measured at 600 GHz and 1.9 THz with a $T_{\text{rec}}^{\text{DSB}}$ of 3600 K at 1.9 THz and an IF

noise bandwidth (NBW) of 6.5 GHz.¹³ A combination of both a low T_{rec}^{DSB} of 930 K at 1.6 THz and a high NBW of 11 GHz in an MgB_2 HEB mixer at 5 K was reported in Ref. 14, which was based on an HPCVD, 5 nm film with a T_c of 31 K. The T_{rec}^{DSB} of this mixer increases by 75% at 20 K. A similar T_{rec}^{DSB} (1000 K) at 1.6 THz together with a NBW of 13 GHz was achieved in Ref. 15. The results in Refs. 13–15 raise the interesting question of whether it is suitable for the operation at 20 K, a temperature which is attractive for space applications because of the availability of the compact, low mass, low dissipation, and space qualified Stirling coolers.¹⁶

MgB_2 HEB mixers are, thus, the alternative to detect, for example, the astrophysically important molecular hydrogen deuteride (HD) line at 2.67 and the neutral atomic oxygen (OI) line at 4.75 THz, which can only be observed from space. However, until now, no sensitivity of such mixers at the frequencies above 2 THz has been reported. Importance of both experimental and theoretical studies at high frequencies (hence, photon energies) is also motivated by the fact that MgB_2 is known to have two families of conduction bands with distinct superconducting gaps,¹⁷ π -band Δ_π and σ -band Δ_σ . It has rather weakly interacting electrons. Photon assisted Cooper pair breaking is an essential part in HEB mixer operation, yet current mixing experimental data with ultra-thin MgB_2 (which can be assessed through HEB performance evaluation) are limited to <2 THz. This is still below the high-gap (σ -) frequency of MgB_2 . The question of the σ -band's role in THz detection/mixing remains open, yet scientifically interesting.

In this Letter, we study an MgB_2 HEB mixer operated at 5.3 THz, which is well above the high-gap frequency. Furthermore, we intentionally increase the T_c of our MgB_2 film to 38.4 K (Ref. 18) by increasing the thickness from 5 nm in Ref. 14 to 7 nm, i.e., close to its maximum theoretical value. The MgB_2 HEBs were fabricated as submicrometer-bridges integrated with a spiral antenna. Our experiment focuses at T_{rec}^{DSB} at 20 K, but the mixer noise temperature (T_m^{DSB}), conversion gain (G_m^{DSB}), and output noise (T_{out}) have also been measured from 6 up to 23 K in order to fully characterize such a new mixer. In addition, its IF noise bandwidth was measured in the frequency range between 0.2 and 14 GHz to characterize it directly at 5.3 THz LO and 20 K.

The HEB used, as shown in the inset (a) of Fig. 1, consists of a 285 nm wide, 850 nm long, and 7 nm thick MgB_2 bridge on a 0.32 mm thick SiC substrate. The narrow bridge is to minimize the HEB volume and hence to reduce the required LO power. The narrow HEB may have a high noise temperature, but it can be operated with an existing far-infrared (FIR) gas laser in the lab. The bridge is connected to a planar spiral antenna consisting of a 195 nm thick Au layer through contact-pads made of an Au layer with a thickness of ≥ 60 nm. The taped contact-pads are designed to reduce the reactance.¹⁹ The antenna is designed to match the HEB impedance of 80 Ω with an upper cutoff frequency of ≥ 6 THz.²⁰ Details of the fabrication of the HEB are described in the [supplementary material](#).

The HEB used (# MgB_2 _BM3_2b) has a normal-state resistance of 51 Ω (defined by the films sheet resistance and the bridge aspect ratio) at above its T_c , which is also the impedance at 5.3 THz.²¹ The HEB has a T_c of 38.4 K and a critical current of 1.3 mA at 5 K, corresponding to a current density of 6.5×10^7 A/cm², which is a factor of 3 higher than what was reported.¹⁴

Figure 2 shows the schematic of our heterodyne measurement setup for measuring the T_{rec}^{DSB} in (a) and for measuring IF bandwidth

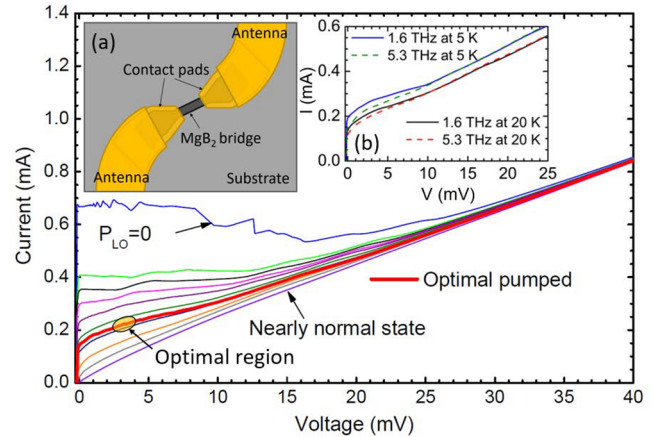


FIG. 1. A set of current-voltage curves of a MgB_2 HEB mixer at 20 K by varying a 5.3 THz LO from zero to fully pumped to the nearly normal state. The yellow circle indicates the optimal operating region for the lowest receiver noise temperature (+5%). At this optimal IV, the required LO power is 9.5 μ W. The inset (a) is an artistic impression of the HEB, which has the exactly same layout as the design. Inset (b) shows a comparison of the pumped IV curves with the same LO power at 1.6 THz and 5.3 THz, which are measured at 5 and 20 K, respectively.

in (b). The LO is the far-infrared (FIR) gas laser at 5.25 THz, and the vacuum setup²² is to avoid the high air absorption loss at 5.25 THz. A heater is installed on the mixer block to elevate the local temperature of the mixer. The components in the IF chain have wide bandwidth (up to 14 GHz) to measure the IF bandwidth of the device. The detailed description of the measurement setup can be found in the [supplementary material](#).

Table I summarizes the optical loss ($1/G_{opt}$) at 5.25 THz in the optical path from the hot/cold loads to the HEB, which includes the Mylar beam splitter (BS), the multimesh low pass filter with a cutoff frequency of 5.8 THz acting as a heat filter, the Si lens, and the power coupling from antenna to the HEB. The Si lens used²³ has an antireflection (AR) coating but designed for 1.6 THz. The optical loss of the AR coated Si lens is simulated using COMSOL Multiphysics by taking the absorption coefficients of parylene-C of 27 cm⁻¹ at 5.25 THz into consideration.^{24,25} The power loss from the antenna to the HEB is found to be 0.94 dB due to the lower HEB resistance (51 Ω) and is 0.31 dB more than the matched case.²⁰

Figure 1 shows a set of current-voltage (IV) curves of the HEB from zero to fully pumped by the 5.3 THz LO, recorded at 20 K. Within the optimal operating region (2.5–4 mV and 0.19–0.25 mA), the T_{rec}^{DSB} of the HEB, to be described, only increases $\sim 5\%$ from its lowest value. From the optimally pumped IV, we derive the LO power of 9.5 μ W at the HEB using the isothermal technique,²⁶ implying a power of ≥ 0.5 mW from the FIR laser. Such a power can be provided by quantum cascade lasers, e.g., 50 mW.²⁷

The T_{rec}^{DSB} of the mixer is obtained by using the Y-factor technique. The receiver output powers of the mixer responding to the hot (P_{hot}) and cold loads (P_{cold}) are measured, and the ratio between these two is the Y-factor. Combining the Y-factor and the Callen–Welton temperatures of the loads, a T_{rec}^{DSB} can be obtained.²² The P_{hot} and P_{cold} are scanned as a function of the HEB current at different DC biased voltages, where the current reflects the scan of the LO power by the

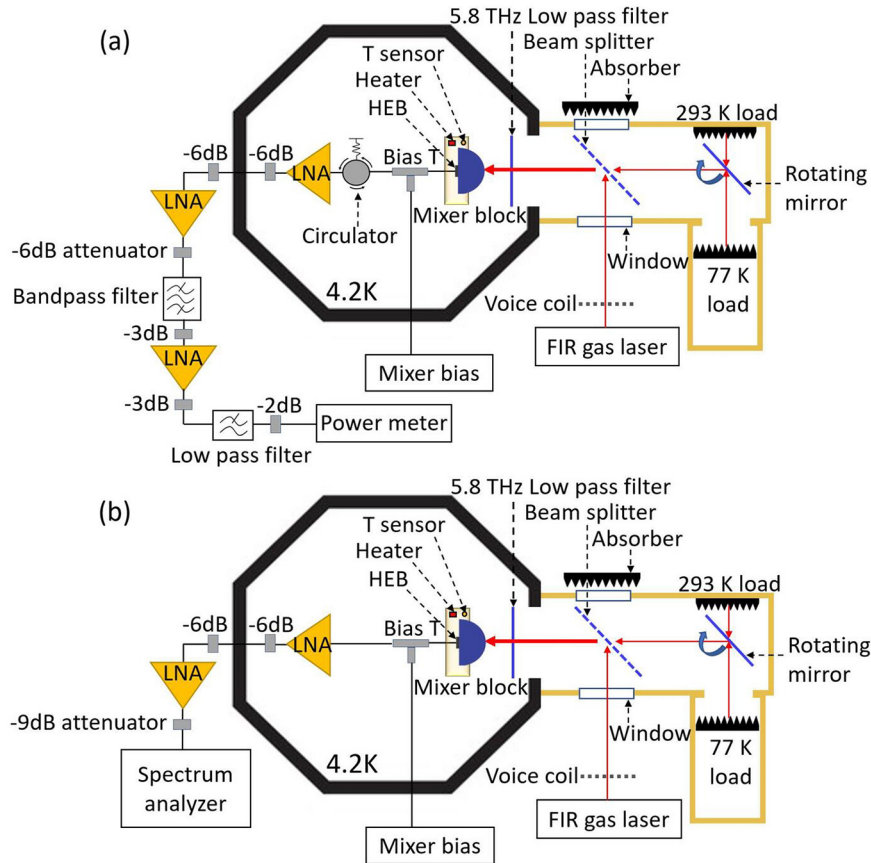


FIG. 2. Schematic of the measurement setup for measuring the T_{rec}^{DSB} in (a) and for measuring IF bandwidth in (b). The hot/cold loads and the beam filter are placed in a vacuum enclosure, attached to the cryostat. A rotating mirror is used to switch between hot and cold loads. The 5.8 THz low pass filter functions as a heat filter.

voice coil attenuator. In this way, the T_{rec}^{DSB} is not influenced by the fluctuations of the LO power and by the direct detection effect.^{2,22} The latter is negligible in our case, because the required LO power ($9.5 \mu\text{W}$) is three orders of magnitude higher than the RF power ($\sim 10 \text{ nW}$) that is the difference between the hot and cold loads. This is confirmed by the fact that we have not seen any shifts in pumped IV curves when the HEB faces two loads. Figure 3 plots the P_{hot} and P_{cold} as a function of the current at the fixed bias voltage of 2.5 mV, measured at 20 K, and their polynomial fitted curves. The latter are used to determine the T_{rec}^{DSB} , plotted in the same figure, from which we select the minimum T_{rec}^{DSB} . We have carried out such measurements at a number of bias voltages ranging from 1 to 7 mV to obtain the minimal T_{rec}^{DSB} at each bias voltage. The results are summarized in the inset of Fig. 3. The lowest T_{rec}^{DSB} is 3960 K when the HEB is biased at 2.5 mV and 0.21 mA.

The T_{rec}^{DSB} can be broken down to its constituents with the following expression:²

$$T_{rec}^{DSB} = T_{opt} + \frac{T_m^{DSB}}{G_{opt}} + \frac{T_{IF}}{G_{opt}G_m^{DSB}}, \quad (1)$$

$$T_m^{DSB} = \frac{T_{out}}{G_m^{DSB}}, \quad (2)$$

where T_{opt} is the noise temperature contribution of the optics ($=137 \text{ K}$) and T_{IF} is the noise temperature of the IF chain ($=4.7 \text{ K}$). For simplicity, the contribution of the quantum noise is not included.²⁸ Furthermore, the T_m^{DSB} is determined by T_{out} and G_m^{DSB} through Eq. (2).

The measured T_{rec}^{DSB} could be improved to 2920 K if we would apply a Si lens with an AR coating optimized for 5.3 THz and utilize a

TABLE I. Loss of the components in the optical path from the hot/cold loads to the HEB at 5.25 THz, including the mylar beam splitter (BS) (L_{BS}) at 300 K, the 5.8 THz low pass filter (L_{filter}) at 4 K, the coated Si lens (L_{lens}) at 4 K, and the coupling between antenna and HEB. The measured T_{rec}^{DSB} together with an expected one if two components are optimized.

| | L_{BS} (dB) | L_{filter} (dB) | L_{lens} (dB) | $L_{coup.}$ (dB) | T_{rec}^{DSB} (K) |
|--|---------------|-------------------|-----------------|------------------|---------------------|
| 6 μm BS and unoptimized coated lens | 1.4 | 0.81 | 0.92 | 0.94 | 3960 |
| 3 μm BS and optimized coated lens | 0.71 | 0.81 | 0.32 | 0.94 | 2920 (Estimated) |

thinner beam splitter of $3\ \mu\text{m}$. The detailed reduction of optical loss can be found in Table I, which includes also both measured and expected $T_{\text{rec}}^{\text{DSB}}$.

At the optimal operating point (with the lowest $T_{\text{rec}}^{\text{DSB}}$), the receiver conversion gain ($G_{\text{rec}}^{\text{DSB}} = G_{\text{opt}} \times G_m^{\text{DSB}}$) is measured by using the U-factor,²⁹ which is the ratio between the receiver output power when the HEB is in its operating point and the receiver output power when it is in its superconducting state. The G_m^{DSB} is $-7.6\ \text{dB}$ by subtracting all the optical losses from the $G_{\text{rec}}^{\text{DSB}}$ based on the measured U-factor of $14.3\ \text{dB}$. The T_m^{DSB} is $1470\ \text{K}$, and the T_{out} is $250\ \text{K}$ using Eqs. (1) and (2). We note that the circulator in our setup is crucial to obtain the reliable U-factor, because it prevents the standing waves [see Fig. 5(a)] between the HEB and the low noise amplifier (LNA).

The $T_{\text{rec}}^{\text{DSB}}$ of the same HEB was also measured at $6.5\ \text{K}$. We obtain a $T_{\text{rec}}^{\text{DSB}}$ of $3530\ \text{K}$ at the bias voltage of $2.5\ \text{mV}$, same as at $20\ \text{K}$, but at a slightly lower current ($0.19\ \text{mA}$). Interestingly, the $T_{\text{rec}}^{\text{DSB}}$ is only 12% lower than the value at $20\ \text{K}$. The small difference between 6 and $20\ \text{K}$ should be attributed to the high T_c . The measured G_m^{DSB} is $-6.7\ \text{dB}$ at $6.5\ \text{K}$ and is clearly higher than what was found ($\leq -8.7\ \text{dB}$) from a NbN HEB at $5.3\ \text{THz}$ at $4\ \text{K}$.²⁸ In contrast, the difference of $T_{\text{rec}}^{\text{DSB}}$ between 5 and $20\ \text{K}$ was much larger and was 75% for a HEB with a T_c of $31\ \text{K}$.¹⁴

To understand the origin of the slow increase in $T_{\text{rec}}^{\text{DSB}}$ from 6 to $20\ \text{K}$, we measured both $T_{\text{rec}}^{\text{DSB}}$ and G_m^{DSB} of the HEB fixed at the biasing point of $2.5\ \text{mV}$ and $0.19\ \text{mA}$ by varying the temperature from 6.5 to $22.5\ \text{K}$. To keep the same biasing point, the LO power has to be reduced with increasing the temperature by about $2\ \mu\text{W}$. Since we focus on the operating at $20\ \text{K}$, we discuss the data only up to this temperature. We find a very similar temperature dependence between $T_{\text{rec}}^{\text{DSB}}$ and T_m^{DSB} (Fig. 4), where there is an increase in 18% for $T_{\text{rec}}^{\text{DSB}}$ (between 6.5 and $20\ \text{K}$), while 19% for T_m^{DSB} . The ratio of the absolute value of the increase, $656\ \text{K}$ for $\Delta T_{\text{rec}}^{\text{DSB}}$ and $249\ \text{K}$ for ΔT_m^{DSB} , can be explained by the G_{opt} ($4.1\ \text{dB}$). However, both $T_{\text{rec}}^{\text{DSB}}$ and T_m^{DSB} remain nearly constant below $10\ \text{K}$.

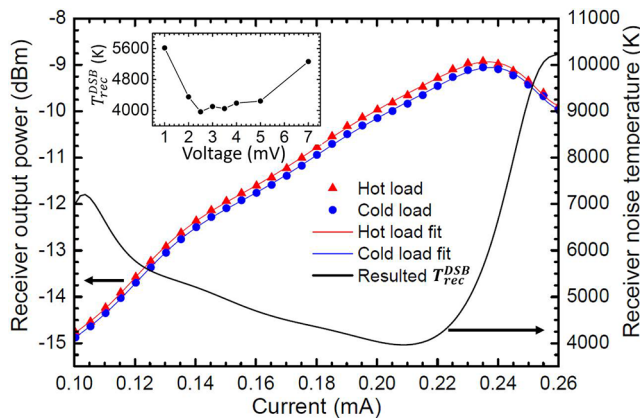


FIG. 3. Measured receiver output power (left axis) of the MgB_2 HEB in response to hot/cold loads, together with the polynomial fits (in a solid line) as a function of the current and the resulted receiver noise temperature (right axis) when it is operated with an LO at $5.3\ \text{THz}$ and at $20\ \text{K}$, and biased at $2.5\ \text{mV}$. The lowest noise temperature is $3960\ \text{K}$. The inset shows the minimum receiver noise temperature from such measurements for different bias voltages, varying from 1 to $7\ \text{mV}$.

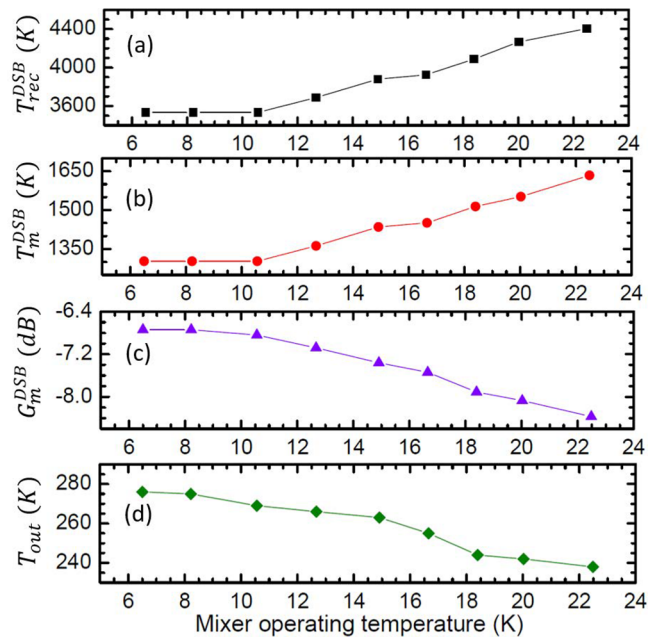


FIG. 4. Measured receiver noise temperature $T_{\text{rec}}^{\text{DSB}}$ (at $1.7\ \text{GHz}$) in (a), derived mixer noise temperature T_m^{DSB} in (b), measured mixer conversion gain G_m^{DSB} in (c), and derived output noise temperature T_{out} in (d) of the MgB_2 HEB mixer as a function of the operating temperature.

In essence, the temperature dependence of T_m^{DSB} originates from G_m^{DSB} and T_{out} both of which decrease with increasing temperature, as shown in Fig. 4. Furthermore, the G_m^{DSB} decreases faster than the T_{out} , leading to the increase in T_m^{DSB} with the temperature according to Eq. (2). Such temperature dependences are relatively unexplored experimentally although the dependence with the very limited number of data points was reported in Ref. 30. In theory, one expects a decrease in T_{out} by increasing the operating temperature based on the hotspot model,^{31–33} because a bell-shaped electron temperature (T_e) profile along an HEB at a lower temperature becomes a flat one by increasing the temperature up to T_c but simultaneously decreasing the LO power for the fixed bias point. The flat T_e profile results in a lower effective T_e in the center of the HEB, which in turn decreases T_{out} since T_{out} is dominated by the thermal fluctuation noise ($\propto T_e^2$). With regard to G_m^{DSB} , one also expects it to decrease with increasing the temperature because of the T_e profile and the reduced LO power. The behavior in our case is qualitatively in line with the simulation reported in Ref. 33.

The IF NBW of the HEB can be obtained from $T_{\text{rec}}^{\text{DSB}}$ measurements in a wide IF range. Figure 5(a) shows the P_{hot} and P_{cold} measured over an IF range of 0.2 – $14\ \text{GHz}$, from which the $T_{\text{rec}}^{\text{DSB}}$ is derived and plotted as a function of IF in Fig. 5(b). The equation, $T_{\text{rec}}^{\text{DSB}}(f) = T_0 [1 + (f/\text{NBW})^2]$, is used to fit the $T_{\text{rec}}^{\text{DSB}}$ data to obtain an NBW, which is $9.5\ \text{GHz} \pm 1\ \text{GHz}$. We believe the low signal-to-noise ratio at the IF can affect the absolute value. As a confirmation, we find the NBW of $11\ \text{GHz} \pm 1\ \text{GHz}$, of the same HEB at $1.63\ \text{THz}$ LO and at $5\ \text{K}$, which agrees to the reported result.¹⁴ The large fluctuations of P_{hot} and P_{cold} highlighted around $8\ \text{GHz}$ in the inset in (a), result in the larger peak/dip in (b), which is believed to be a technical issue in the IF chain but not from the HEB.

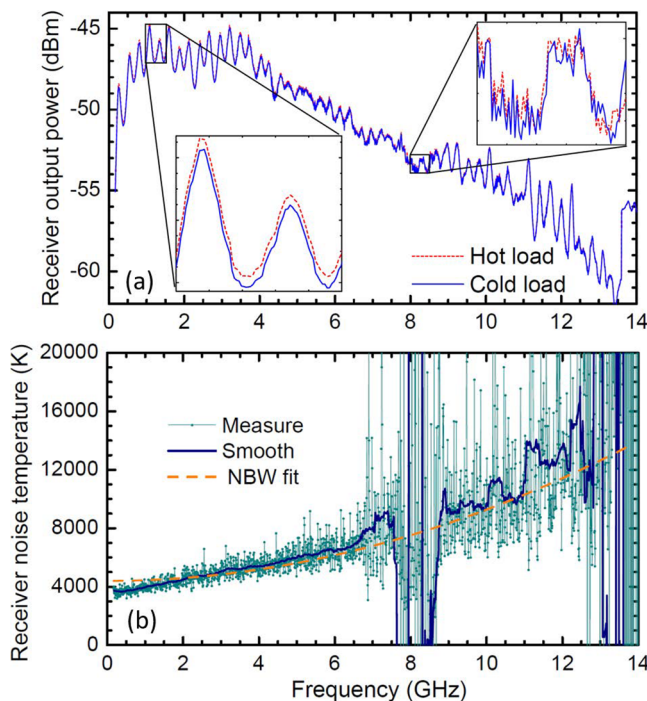


FIG. 5. (a) Measured receiver output powers of the MgB_2 HEB corresponding to hot and cold loads as a function of the intermediate frequency (IF) when it is in its optimal operating point and at 20 K. The inset zooms in the frequency range of 1–1.5 and 8–8.5 GHz. (b) Receiver noise temperature as a function of IF. The orange line is the best fit of $T_{\text{rec}}^{\text{DSB}}(f) = T_0 [1 + (f/\text{NBW})^2]$ to the data, where the NBW, noise bandwidth, is 9.5 GHz.

The $\Delta_\pi = 1.8$ meV and $\Delta_\sigma = 6.3$ meV of MgB_2 were reported for a T_c of 38.7 K,¹⁷ corresponding to the gap frequency of 0.87 and 3.05 THz, respectively. Assuming these two gap frequencies apply also to our HEB since our T_c is 38.4 K, one would expect a different pumped IV when it is at 5.3 THz, where the THz photons can break all the Cooper-pairs and can be uniformly absorbed, and when it is at 1.6 THz, the photons can only break the Cooper-pairs in the π -band and can, thus, be non-uniformly absorbed. Inset (b) in Fig. 1 shows pumped IV curves at 1.6 and 5.3 THz measured at 5 and 20 K, respectively, where the IV at 5.3 THz has a lower current than that at 1.6 THz at the low bias voltages. This effect, as one would expect, is stronger at 5 K, while the two IV curves are exactly the same at the high voltages. The latter suggests that the pumped LO power is the same. The effect is analogous to the NbN HEB operated below and above its gap frequency, where the IV curves at two LO frequencies differ at low voltages.³⁴ In addition, the G_m^{DSB} at 1.6 THz is found to be slightly lower than that at 5.3 THz, which may further support that the double-gap effect plays a role in our experiment. The double-gap effect could be present in pumped IV of the MgB_2 HEB between 1.6 and 2.5 THz in Ref. 12 although the 2.5 THz is too close to the high gap frequency.

The measured $T_{\text{rec}}^{\text{DSB}}$ will increase by less than 2% and, thus, remain nearly unchanged if the LNA is also operated at 20 K, where T_{IF} will increase from 4.7 to 8.5 K. To compare the sensitivity of our HEB with the reported value (930 K) at 1.6 THz only,¹⁴ we also

measured a $T_{\text{rec}}^{\text{DSB}}$ of the same HEB at 1.6 THz and at 6.5 K and obtained 2100 K, which is higher and is likely due to the narrower bridge width.³⁵

The sensitive MgB_2 HEB mixer with a large NBW, which can be operated at 20 K in a Stirling cooler,¹⁶ is promising for space applications. Based on the measured 3960 K, the expected, lowest $T_{\text{rec}}^{\text{DSB}}$ of 2720 K at 5.3 THz by using the optimized coating lens ($\rightarrow 3470$ K), the thinner beam splitter ($\rightarrow 2920$ K), and also the antenna matched HEB resistance ($\rightarrow 2720$ K), is 28 times lower than a Schottky diode mixer at 4.7 THz³⁶ but is only about 2.5 times more than an NbN HEB mixer at 5.3 THz.²⁰

In summary, we have demonstrated a low noise MgB_2 HEB mixer operated at 5.3 THz LO and at 20 K. The measured receiver noise temperature, $T_{\text{rec}}^{\text{DSB}}$, is 3960 K, which can be further decreased to 2920 K for the same device by using an optimized coated lens and a 3 μm beam splitter. The $T_{\text{rec}}^{\text{DSB}}$ has a weak temperature dependence because of the high T_c and has only 12% decrease in the optimal value when it reaches 6.5 K or below. The measured IF NBW is 9.5 GHz at 20 K. Additionally, the temperature dependences of the mixer conversion gain and output noise have been studied by varying the operating temperature from 6 to 23 K. Finally, we observed different IV curves at low bias voltages, pumped at 1.6 and 5.3 THz, suggesting the presence of the two superconducting gaps in the thin MgB_2 .

See the [supplementary material](#) for the following: part A: the fabrication process of MgB_2 HEBs and part B: the description of the heterodyne measurement setup.

We thank P. Khosropanah and A. Aminaei for their useful discussions and inputs, and W. Laauwen, W.-J. Vreeling, B. Kramer, and H. Ode at SRON, and R. C. Horsten at TU Delft for their valuable technical supports. The work at Chalmers University of Technology was supported by the Swedish Research Council (No. 2019-04345) and the Swedish National Space Agency (No. 198/16). Y. Gan is funded partly by the China Scholarship Council (CSC) and partly by the University of Groningen.

AUTHOR DECLARATIONS

Conflict of Interest

The authors have no conflicts to disclose.

DATA AVAILABILITY

The data that support the findings of this study are available from the corresponding author upon reasonable request.

REFERENCES

- ¹E. M. Gershenzon, G. N. Gol'tsman, I. G. Gogidze, Y. P. Gusev, A. I. Elant'ev, B. S. Karasik, and A. D. Semenov, *Sov. Phys. Supercond.* **3**, 1582 (1990).
- ²H.-W. Hubers, *IEEE J. Sel. Top. Quantum Electron.* **14**, 378 (2008).
- ³F. F. S. van der Tak, S. C. Madden, P. Roelfsema, L. Armus, M. Baes, J. Bernard-Salas, A. Bolatto, S. Bontemps, C. Bot, C. M. Bradford, J. Braine, L. Ciesla, D. Clements, D. Cormier, J. A. Fernández-Ontiveros, F. Galliano, M. Giard, H. Gomez, E. González-Alfonso, F. Herpin, D. Johnstone, A. Jones, H. Kaneda, F. Kemper, V. Lebouteiller, I. D. Looze, M. Matsuura, T. Nakagawa, T. Onaka, P. Pérez-González, R. Shipman, and L. Spinoglio, *Publ. Astron. Soc. Aust.* **35**, e002 (2018).
- ⁴C. Risacher, R. Gusten, J. Stutzki, H.-W. Hubers, D. Buchel, U. Graf, S. Heyminck, C. E. Honingh, K. Jacobs, B. Klein, T. Klein, C. Leinz, P. Putz, N.

- Reyes, O. Ricken, H.-J. Wunsch, P. Fusco, and S. Rosner, *IEEE Trans. Terahertz Sci. Technol.* **6**, 199 (2016).
- ⁵D. J. Hayton, J. L. Kloosterman, Y. Ren, T. Kao, J. N. Hovenier, J. R. Gao, T. N. Klapwijk, Q. Hu, C. K. Walker, and J. L. Reno, *Proc. SPIE* **9153**, 91531R-1 (2014).
- ⁶T. de Graauw, F. Helmich, T. Phillips, J. Stutzki, E. Caux, N. D. Whyborn *et al.*, *Astron. Astrophys.* **518**, L6 (2010).
- ⁷J. L. Kloosterman, D. J. Hayton, Y. Ren, T. Y. Kao, J. N. Hovenier, J. R. Gao, T. M. Klapwijk, Q. Hu, C. K. Walker, and J. L. Reno, *Appl. Phys. Lett.* **102**, 011123 (2013).
- ⁸H. Linz, H. Beuther, M. Gerin, J. R. Goicoechea, F. Helmich, O. Krause, Y. Liu, S. Molinari, V. Ossenkopf-Okada, J. Pineda, M. Sauvage, E. Schinnerer, F. van der Tak, M. Wiedner, J. Amiaux, D. Bhatia, L. Buinhas, G. Durand, R. Förstner, U. Graf, and M. Lezius, *Exp. Astron.* **51**, 661–697 (2021).
- ⁹J. Waters, L. Froidevaux, R. Harwood, R. Jarnot, H. Pickett, W. Read *et al.*, *IEEE Trans. Geosci. Remote Sens.* **44**, 1075 (2006).
- ¹⁰P. Canfield and G. Crabtree, *Phys. Today* **56**(3), 34 (2003).
- ¹¹S. Cherednichenko, V. Drakinskiy, K. Ueda, and M. Naito, *Appl. Phys. Lett.* **90**, 023507 (2007).
- ¹²D. Cunnane, J. H. Kawamura, M. A. Wolak, N. Acharya, T. Tan, X. X. Xi, and B. S. Karasik, *IEEE Trans. Appl. Supercond.* **25**, 2300206 (2015).
- ¹³D. Cunnane, J. H. Kawamura, M. A. Wolak, N. Acharya, X. X. Xi, and B. S. Karasik, *IEEE Trans. Appl. Supercond.* **27**, 2300405 (2017).
- ¹⁴E. Novoselov and S. Cherednichenko, *Appl. Phys. Lett.* **110**, 032601 (2017).
- ¹⁵N. Acharya, E. Novoselov, and S. Cherednichenko, *IEEE Trans. Terahertz Sci. Technol.* **9**, 565 (2019).
- ¹⁶D. M. A. Aminou, J. Bézy, R. Meynart, P. Blythe, S. Kraft, I. Zayer, M. Linder, M. Falkner, and H. Luhmann, *Proc. SPIE* **7474**, 747407 (2009).
- ¹⁷M. Putti, M. Affronte, C. Ferdeghini, P. Manfrinetti, C. Tarantini, and E. Lehmann, *Phys. Rev. Lett.* **96**, 077003 (2006).
- ¹⁸E. Novoselov, N. Zhang, and S. Cherednichenko, *IEEE Trans. Appl. Supercond.* **27**, 4601605 (2017).
- ¹⁹P. Focardi, A. Neto, and W. R. McGrath, *IEEE Trans. Microwave Theory Tech.* **50**, 2374 (2002).
- ²⁰W. Zhang, P. Khosropanah, J. R. Gao, T. Bansal, T. M. Klapwijk, W. Miao, and S. C. Shi, *J. Appl. Phys.* **108**, 093102 (2010).
- ²¹E. L. Kollberg, K. S. Yngvesson, Y. Ren, W. Zhang, P. Khosropanah, and J. Gao, *IEEE Trans. Terahertz Sci. Technol.* **1**, 383 (2011).
- ²²P. Khosropanah, J. R. Gao, W. M. Laauwen, and M. Hajenius, *Appl. Phys. Lett.* **91**, 221111 (2007).
- ²³We use an elliptical Si lens with the semi-minor axis of the ellipse a of 5 mm, the semi-major axis b of 5.235 mm, and the extension c from geometric center of the lens of 1.2 mm thick Si and 0.32 mm thick SiC substrate. This combination forms a nearly perfect elliptical lens based on the simulation by COMSOL Multiphysics. The refractive index is 3.38 for Si and 3.14 for SiC.
- ²⁴Y. Gan, B. Mirzaei, S. van der Poel, J. R. G. Silva, M. Finkel, M. Eggens, M. Ridder, A. Khalatpour, Q. Hu, F. van der Tak, and J. Gao, *Opt. Express* **28**, 32693 (2020).
- ²⁵A. J. Gatesman, J. Waldman, M. Ji, C. Musante, and S. Yagvesson, *IEEE Microwave Guided Wave Lett.* **10**, 264 (2000).
- ²⁶H. Ekström, B. S. Karasik, E. K. erg, and K. S. Yngvesson, *IEEE Trans. Microwave Theory Tech.* **43**, 938 (1995).
- ²⁷A. Khalatpour, J. L. Reno, and Q. Hu, *Nat. Photonics* **13**, 47 (2019).
- ²⁸W. Zhang, P. Khosropanah, J. R. Gao, E. L. Kollberg, K. S. Yngvesson, T. Bansal, R. Barends, and T. M. Klapwijk, *Appl. Phys. Lett.* **96**, 111113 (2010).
- ²⁹S. Cherednichenko, M. Kroug, H. Merkel, P. Khosropanah, A. Adam, E. Kollberg, D. Loudkov, G. Gol'tsman, B. Voronov, H. Richter, and H. Huebers, *Physica C* **372–376**, 427 (2002).
- ³⁰E. Novoselov and S. Cherednichenko, *IEEE Trans. Terahertz Sci. Technol.* **7**, 704 (2017).
- ³¹D. W. Floet, E. Miedema, T. M. Klapwijk, and J. R. Gao, *Appl. Phys. Lett.* **74**, 433 (1999).
- ³²H. F. Merkel, P. Khosropanah, D. W. Floet, P. A. Yagoubov, and E. L. Kollberg, *IEEE Trans. Microwave Theory Tech.* **48**, 690 (2000).
- ³³W. Miao, W. Zhang, K. M. Zhou, H. Gao, K. Zhang, W. Y. Duan, Q. J. Yao, S. C. Shi, Y. Delorme, and R. Lefevre, *IEEE Trans. Appl. Supercond.* **27**, 2200304 (2017).
- ³⁴W. Miao, W. Zhang, J. Q. Zhong, S. C. Shi, Y. Delorme, R. Lefevre, and A. Feret, *Appl. Phys. Lett.* **104**, 052605 (2014).
- ³⁵E. Novoselov, “MgB₂ hot-electron bolometer mixers for sub-mm wave astronomy,” Ph.D. thesis (Chalmers University of Technology, Sweden, 2014).
- ³⁶I. Mehdi, J. V. Siles, C. Lee, and E. Schlecht, *Proc. IEEE* **105**, 990 (2017).